



## ORIENTATION-INDEPENDENT MEASURES OF GROUND MOTION FOR A DATABASE OF CENTRAL AMERICA

D.A. Hidalgo-Leiva<sup>(1)</sup>, L.G. Pujades<sup>(2)</sup>, S.A. Díaz<sup>(3)</sup>, A.H. Barbat<sup>(4)</sup>, J.R. González-Drigo<sup>(5)</sup>

<sup>(1)</sup> PhD Candidate, Polytechnic University of Catalonia, School of Civil Engineering, Department of Civil and Environmental Engineering (DECA). Division of Geotechnical Engineering and Geo-Sciences, [diego.hidalgo@upc.edu](mailto:diego.hidalgo@upc.edu)

<sup>(2)</sup> Full Professor, Polytechnic University of Catalonia, School of Civil Engineering, Department of Civil and Environmental Engineering (DECA). Division of Geotechnical Engineering and Geo-Sciences, [lluis.pujades@upc.edu](mailto:lluis.pujades@upc.edu)

<sup>(3)</sup> Professor, Universidad Juarez Autonoma de Tabasco (UJAT), México. Now at: PhD candidate, DECA-ETCG, UPC Barcelona Tech, Spain. [sergio.alberto.diaz@upc.edu](mailto:sergio.alberto.diaz@upc.edu)

<sup>(4)</sup> Full Professor, Polytechnic University of Catalonia, School of Civil Engineering, Department of Civil and Environmental Engineering (DECA). Division of structural analysis, [alex.barbat@upc.edu](mailto:alex.barbat@upc.edu)

<sup>(5)</sup> Full Professor, Polytechnic University of Catalonia, School of Civil Engineering, Department of Civil and Environmental Engineering (DECA). Division of Geotechnical Engineering and Geo-Sciences, [jose.ramon.gonzalez@upc.edu](mailto:jose.ramon.gonzalez@upc.edu),

### **Abstract**

Ground Motion Prediction Equations commonly use response spectra as input data. However, the selection of a unique spectral function which minimizes the error between predicted and observed values, remains a subject of research. Recently, response spectra independent of the sensors orientation have been used in seismic hazard studies, showing a reduction in the error of the predictive equations. Nevertheless, the use of response spectra determined from the geometric mean of the horizontal orthogonal response spectra is in debate. In particular, when it is convenient to know about the maximum spectral accelerations expected. In this paper, different Orientation-Independent Measures are calculated for a Strong Motion Data Base of Central America. A total of 1406 strong motion records with 3 orthogonal acceleration time series are used. For this database, the median value of the ratio between the maximum spectral response with orientation of the sensors independence and the one of the geometric mean of the as-recorded spectral response varies as a function of the period, with a minimum of 1.22 at 0.1 seconds and a maximum of 1.3 at periods greater than 1 second. A new approach, for determining the maximum Orientation-Independent spectral response, which is based on the Root-Sum-of-Squares, is probed.

*Keywords: Directionality; Ground Motion Equations; Seismic Response.*

## 1. Introduction

Ground motion prediction equations (GMPE) play an important role in seismic hazard assessment and, consequently, in structural seismic design. Commonly, the GMPEs are defined as a combination of parameters based on the acceleration response spectrum of two horizontal components of earthquakes records. A review of the different combinations used and published GMPEs are presented in Douglas [1]. According to this review, the most used parameter is the Geometric Mean of the response spectra of the two as-recorded components ( $Sa_{GMar}$ ).

Historically,  $Sa_{GMar}$  has been preferred to determine the expected value of response spectra for GMPE due to a reduction of the aleatory uncertainty when compared with other Intensity Measures (IM). This reduction is obtained through a regression analysis [2,3,4]. Using the as-recorded orientation of the ground motion makes the IM dependent of this aleatory orientation, which is often aligned with the cardinal directions or with the normal (transversal) and parallel (longitudinal) orientations of specific structures. In recent years, different methods have been proposed to determine orientation independent parameters [5,6,7], having a significant impact on the selection of response parameters for the GMPEs. They were developed by, for instance, the Pacific Earthquake Engineering Research Center (PEER), firstly in the 2008 versions, where a IM based on the geometric-mean, but with rotational independence, was used [8] and, afterwards, in the 2012 version, using the non-geometric-mean IM with rotational independence [9].

In this paper, a new angle and period independent parameter based on the root-sum-of-squares is proposed. Besides, a database of accelerograms recorded in Central America [10] is analyzed and used to determine different ratios between median and maximum IM.

## 2. Orientation-Independent Measure

In this section the basic definitions and an example of the most well-known measures that take into account the influence of the orientation of the recording devices are presented. The orientation-independent measures are desirable on the assumption that, by eliminating this dependency, a source of epistemic uncertainty is removed. The  $Sa_{GMar}$  is the most frequent parameter used in the ground motion prediction equations [1]. If  $Sa_x$  and  $Sa_y$  are the response spectra of the as recorded time series  $acc_x$  and  $acc_y$  respectively,  $Sa_{GMar}$  is the geometric mean of this two response spectrum. This parameter has two different sources of uncertainty, the first one is related to the dependency on the orientation of the sensors and the polarization of the signal and the second one, concerns to the process for obtaining it, since the computations of  $Sa_{GMar}$  (as others parameters) usually average spectral quantities which implies the combination of two maximum values without considering the time mismatch in the time series of the response itself.

To eliminate the dependence of IM on as-recorded orientation, Boore et al.[5] proposed the  $Sa_{GMRotDpp}$  and  $Sa_{GMRotIpp}$  IM's, which are orientation-independent. To determine  $Sa_{GMRotDpp}$ , it is necessary to compute the geometric-mean of the response spectra for all orthogonal components of the ground motion for a specified period, considering the input signals as is defined in Eq. (1) and (2). Taking a constant angular increment ( $\Delta\theta=1^\circ$ ), a total of 90 independent values are obtained for each period, and then by selecting the desired percentile (pp=50 for median value and pp=100 for maximum value) the IM is defined.  $Sa_{GMRotDpp}$  uses the geometric-mean of different orientation at different periods, and therefore is not defined by two particular ground motion time series. The period dependence of  $Sa_{GMRotDpp}$  (D) is defined by a specific rotation angle and it could be different for each  $T_n$ . To obtain period independent measures,  $Sa_{GMRotIpp}$ , is then determined as the geometric-mean of the response spectra for a specific rotation angle, with the smallest difference from the spectrum  $Sa_{GMRotDpp}$ , thru a period range.

$$acc_1(t, \theta) = acc_x(t) \cos \theta + acc_y(t) \sin \theta \quad (1)$$

$$acc_2(t, \theta) = -acc_x(t) \sin \theta + acc_y(t) \cos \theta \quad (2)$$

A second group of IM called  $Sa_{RotDpp}$  and  $Sa_{RotIpp}$ , are based on non-geometric-mean measures with orientation-independence [6]. The period-dependent (D) measure is computed as the response spectrum of a

single component, with a combination of the two as-recorded time series, as defined in Eq. (1). For  $Sa_{RotDpp}$  is necessary the spectral response for all possible orientations, and with an angular increment equal to  $1^\circ$ , creates 180 values for a specific period. The computation of the period-independent (I) measure is identical to the  $Sa_{GMrotDpp}$ , except that the rotation angle range is  $180^\circ$  instead of  $90^\circ$ . In the same way as  $Sa_{GMrotDpp}$ , the 50<sup>th</sup> percentile represent the median value and the 100<sup>th</sup> the maximum value, which in this case represents the maximum response spectra amplitude in all the possible orientations. The Samara (Costa Rica) earthquake of 7.6Mw [11] recorded in the GNSR station on September 5<sup>th</sup> 2012, is used herein to shown the behavior of the different IMs as can be seen in Fig. 1.  $Sa_{RotI100}$  in this case coincides with the N90E direction and although it is difficult to see  $Sa_{RotI50}$  is approximately equal to  $Sa_{RotD100}$  for periods greater than 0.5 seconds, a situation that may occur for a range of periods depending on the record and that was commented by Boore [6].

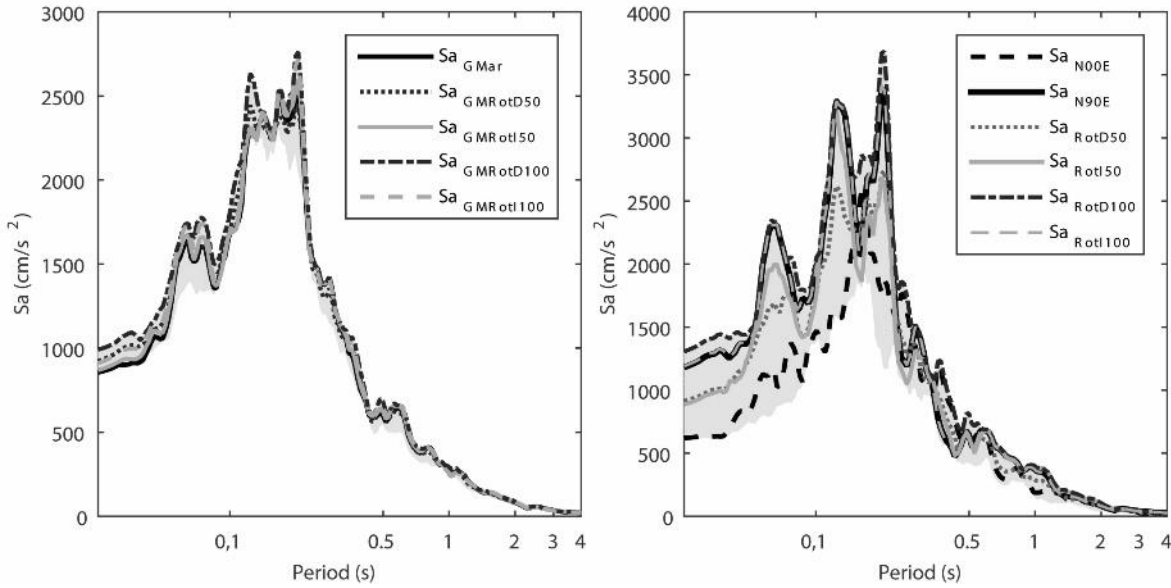


Fig. 1- Response spectra for two acceleration horizontal components of the Samara 7.6 Mw earthquake and for their all non-redundant rotations: a) based on Geometric Mean, b) based on non-Geometric-Mean.

An orientation-independent maximum-response IM is proposed and presented here. This IM is based on the bidirectional response of a damped single-degree-of-freedom (SDOF) system over the horizontal plane (5% of critical damping is assumed throughout). Let denote the total acceleration response in the as-recorded direction of the SDOF system as  $\ddot{u}_{xt}(T_i, t, \xi)$  and  $\ddot{u}_{yt}(T_i, t, \xi)$ , where normally the x-direction corresponds to the N90E azimuth and the y-direction correspond to the N00E azimuth, and both are functions of the SDOF natural period  $T_i$ , and of the critical damping ratio  $\xi$ . By solving the response in acceleration as a vector point-to-point for both times series, the simultaneous modulus and phase of the acceleration vector is obtained as:

$$\ddot{u}_{RSS}(T_i, t, \xi) = \sqrt{[\ddot{u}_{xt}(T_i, t, \xi)]^2 + [\ddot{u}_{yt}(T_i, t, \xi)]^2} \quad (3)$$

$$\theta_{RSS}(T_i, t, \xi) = \tan^{-1} \left[ \frac{\ddot{u}_{yt}(T_i, t, \xi)}{\ddot{u}_{xt}(T_i, t, \xi)} \right] \quad (4)$$

Combining the solution of Eq. (3) and Eq. (4), allows to reconstruct the orbit in acceleration of the SDOF for any record. The ground motion selected to illustrate this procedure was recorded at the GNSR station during the September 5<sup>th</sup> 2012, Mw 7.6 Samara-Costa Rica Earthquake [11]. For each period considered the bidirectional response can be obtained, in the Fig. 2 the response for the oscillators at 0.1 and 1.0 seconds are shown. This solution allows to understand some others parameters, for example, the spectral responses in the orthogonal direction are the maximum value of the projection of all the response points over the N90E and N00E planes. These values have not necessary to coincide with the projection of the maximum response (marked as a circle). This maximum response is defined as the maximal spectral response and is obtained as:

$$Sa_{RSS}(T_i, \xi) = \max |\ddot{u}_{RSS}(T_i, t_i, \xi)| \forall t_i \quad (5)$$

This maximum IM is independent of the axes orientation, and therefore its value is the same for any angular variation of the inputs, and thus, can be obtained from only one pair of time series. With this procedure it is also possible to determine the direction of the maximum response for each period and damping, which in the case of Fig. 2 are 345° and 27° respectively for 0.1 and 1 s periods. This angle is comparable with the one obtained in  $Sa_{RotD100}$  for each  $T_i$ , but without the need of performing the rotational scan of the responses. A similar procedure was proposed by Rupakhety and Sigbjörnsson [7], using the displacement response and the pseudo-acceleration instead of the acceleration response.

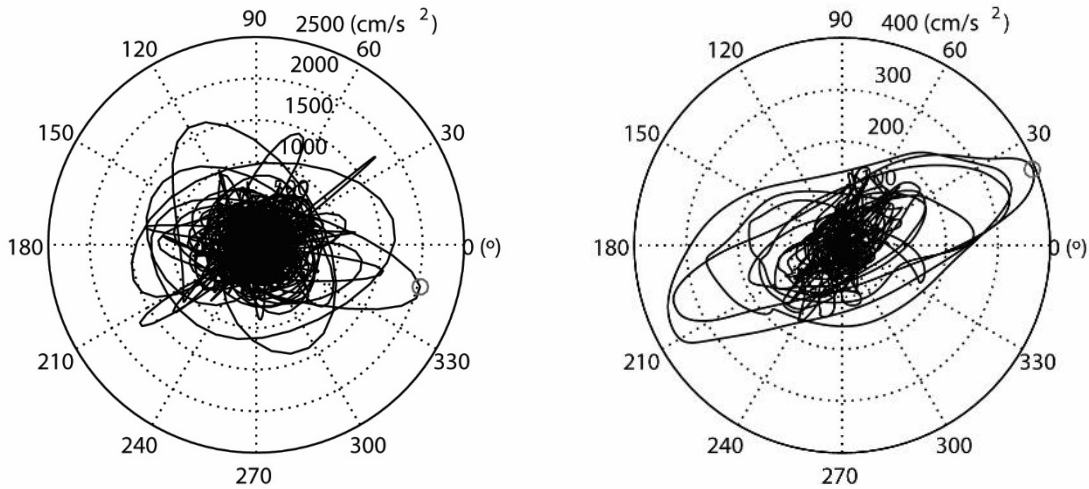


Fig. 2 – Orbit (amplitudes and phases) for the bidirectional acceleration response of a SDOF with: a)  $T_n=0.1$  s, b)  $T_n=1$  s.

### 3. Database description

The database was pretreated and standardized by the Earthquake Engineering Laboratory of the University of Costa Rica (LIS-UCR). The available data and the file formats [12] were corrected, completed and standardized, as described by Schmidt-Diaz [13]. The whole database has 3191 three-component acceleration records corresponding to 1004 earthquakes that were registered between 1961 and 2012. The recording stations are located in the Central American region.

The records come from 5 different seismological centers (two from Costa Rica, two from El Salvador and one from Nicaragua). All the countries are affected by the same seismogenetic features, with a high influence of the subduction zone in the Pacific coast, where the Cocos plate subducts under the Caribbean plate. The distribution of the strong ground motion stations can be seen in the Fig. 3a (for a complete description of the stations characteristics refer to [13,14]) and Fig. 3b shows the epicenter location of the earthquakes with  $M_w > 5.5$ . It can be seen, how the subduction zone generates a correlation between the azimuth from the epicenter with respect to the location of the stations, and therefore, the populated regions.

Table 1 shows a classification of the records according to magnitude, depth, distance and azimuth; a separation between Subduction and Local or intraplate events is also shown. All this information was obtained from the headers of the records. The median magnitude ( $M_w$ ) of the events is 5.2 for subduction and 4.8 for local/intraplate events. Only a few records (144) correspond to great earthquakes with  $M_w$  magnitude higher than 7.0. The parameter used for selecting the record for the analysis was the  $PGA_H$ , defined as the maximum horizontal acceleration of each record without any kind of ponderation. A value of  $10 \text{ cm/s}^2$  was set as the lower limit for considering the records in the directionality analysis; a total of 1410 records fulfilled this criterion.

Moreover, four files from Nicaragua were excluded due to the lack of information in the header. Therefore 1406 files were selected as a first group of records; this group is called DB-01. These records correspond to 451 events (218 subduction and 233 local/intraplate origin).

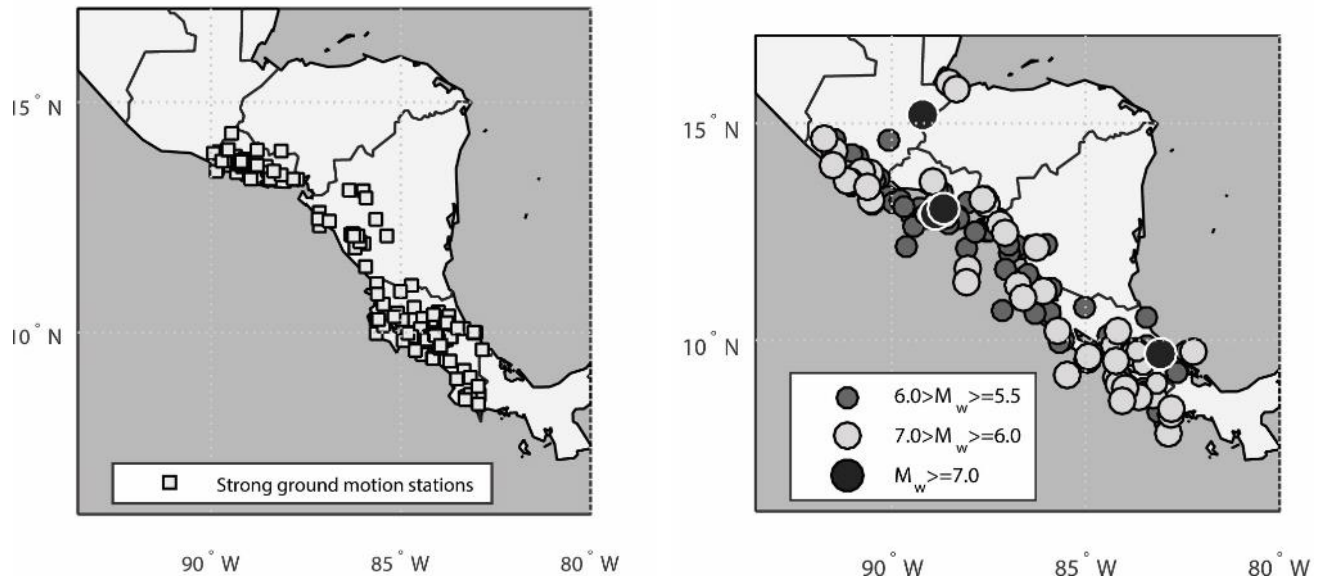


Fig. 3- a) Strong ground motion stations in Costa Rica, El Salvador and Nicaragua, b) Epicenter distribution of selected earthquakes (DB-01 and  $M_w \geq 5.5$ ).

This database has records from different types of accelerometers, which through the years evolved from analogical to digital. Obviously, the quality of old records is lower. An important issue related to the quality of the accelerograms concerns to the useful frequency band that, for old records, is narrower. As it can be seen in Table 2, a large number of files, have a low cut frequency,  $F_L$ , equal to 0.8 Hz (1.25 seconds), limiting the maximum natural period allowed in the calculations of response spectra. Furthermore, assuming that the transfer function of the instrument is flat in the frequency range of interest, the high frequency limit,  $F_H$ , is controlled by the sampling rate. Information in Table 2 has been also taken from the headers of the files.

The acceleration time series were first processed by applying a third order Butterworth bandpass filter with zero-phase shift (processing the input signal in both the forward and reverse directions, doubling the filter order), with frequency corners  $F_H$  of 20 Hz and  $F_L$  equal to the frequency provided in the file header, with a minimum low frequency ( $F_L$ ) of 0.1Hz. For each file, the maximum useful period ( $T_h$ ) is taken as the inverse of the minimum corner frequency of the filter. Some authors [15,16] recommend take a smaller period for  $T_h$  when response spectra are calculated, nevertheless,  $T_h$  is taken as defined above for this paper.

To reduce the number of points of the records, without affecting the strong phase of the signal, the pre and post event samples of each file were examined, determining, for intervals of 5 seconds, the mean value and the root-mean-square-deviation. If the maximum value in the subsequent interval was higher than the 99% (2.5 std. deviations) of the acceleration, then that interval was selected as the initial interval. This procedure is useful especially when accelerograms have a large number of samples recorded before and after the earthquake. Finally, to avoid ripling effects, a Tukey window with a 0.25 factor is applied in the time domain.

When feasible, response spectra were computed at 200 periods uniformly distributed in a logarithmic scale varying from 0.025 to 10 seconds. As  $T_h$  varies for different records, not all of the response spectra have 200 points; the minimum number of periods has been 133 for the cases with  $F_L$  equal to 0.8 Hz.

Table 1 - Summary of statistics for Central America Database, in number of records <sup>(1)</sup>.

Magnitude Mw				Depth (Km)				Epicentral Distance (Km)				Azimuth Ep. to St. (deg)				PGA <sub>H</sub> (cm/s <sup>2</sup> )	
Interv <sup>(2)</sup>	Sub <sup>(3)</sup> (%)	Local <sup>(4)</sup> (%)	Total	Interv <sup>(2)</sup>	Sub <sup>(3)</sup> (%)	Local <sup>(4)</sup> (%)	Total	Interv <sup>(2)</sup>	Sub <sup>(3)</sup> (%)	Local <sup>(4)</sup> (%)	Total	Interv <sup>(2)</sup>	Sub <sup>(3)</sup> (%)	Local <sup>(4)</sup> (%)	Total	Interv <sup>(2)</sup>	Total
<3.0	15 (0.8)	48 (3.9)	63	<10	26 (1.3)	539 (44.1)	565	<10	20 (1.0)	182 (14.9)	202	0-60	641 (32.6)	231 (18.9)	872	<10	1781
3.0-4.0	104 (5.3)	219 (17.9)	323	10-25	292 (14.8)	538 (44.0)	830	10-25	62 (3.2)	272 (22.2)	334	60-120	448 (22.8)	270 (22.1)	718	10-20	570
4.0-5.0	661 (33.6)	389 (31.8)	1050	25-50	852 (43.3)	139 (11.4)	991	25-50	295 (15.0)	215 (17.6)	510	120-180	62 (3.2)	115 (9.4)	177	20-50	523
5.0-6.0	850 (43.2)	360 (29.4)	1210	50-100	756 (38.4)	7 (0.6)	763	50-100	933 (47.4)	216 (17.7)	1149	180-240	38 (1.9)	154 (12.6)	192	50-100	199
6.0-7.0	239 (12.1)	162 (13.2)	401	100-150	24 (1.2)	0 (0.0)	24	100-150	335 (17.0)	171 (14.0)	506	240-300	59 (3.0)	189 (15.5)	248	100-250	98
>7.0	99 (5.0)	45 (3.7)	144	>150	18 (0.9)	0 (0.0)	18	>150	323 (16.4)	167 (13.7)	490	300-360	720 (36.6)	264 (21.6)	984	250>	20
Total	1968	1223	3191	Total	1968	1223	3191	Total	1968	1223	3191	Total	1968	1223	3191	Total	3191

	Magnitude Mw			Depth (Km)			Epicentral Distance (Km)			Azimuth Ep. to St. (deg)			PGA <sub>H</sub> (cm/s <sup>2</sup> )
	Sub <sup>(3)</sup>	Local <sup>(4)</sup>	Total	Sub <sup>(3)</sup>	Local <sup>(4)</sup>	Total	Sub <sup>(3)</sup>	Local <sup>(4)</sup>	Total	Sub <sup>(3)</sup>	Local <sup>(4)</sup>	Total	Total
<b>Mode</b>	4.7	4.2	5.4	50	10	50	33.75	17.22	17.22	0.1	223.3	0.1	11.3
<b>Median</b>	5.2	4.8	5.2	44.7	10	29.2	82.28	40.86	73.2	105.9	179.2	120.9	22,1
<b>Mean</b>	5.22	4.85	5.08	46.42	12.5	33.43	101.82	70.56	89.84	169.1	179.2	173.0	7,7
<b>Std.</b>	0.92	1.1	1.01	25.94	9.42	26.84	80.64	72.91	79.23	137.3	113.9	128.9	59,5

<sup>(1)</sup> Records: file with three orthogonal components for each seismic event. Usually there are more than one record for each event, depending on the number of recording stations.

<sup>(2)</sup> Interval or range of values used in the classification.

<sup>(3)</sup> Sub (Subduction or Interface): Earthquakes occurred along the interfaces between the Cocos and the Caribbean Plates. Generally, they have focal mechanisms consistent with its occurrence with reverse shift in diving planes.

<sup>(4)</sup> Local or Intraplate: Earthquakes occurred inside the Caribbean Plate associated to internal deformation, generally they have focal mechanisms consistent with normal faults, caused by displacement in extension.

Table 2 – Frequency filters applied in preprocess of database.

$F_L$ (Hz)	Original DB (%)	DB-01 (%)	$F_H$ (Hz)	Original DB (%)	DB-01 (%)
0,10	1773 (55.6)	621 (44,17)	23	443 (13.9)	408 (29,02)
0,12	815 (25.5)	237 (16,86)	25	50 (1.57)	46 (3,27)
0,25	50 (1.57)	46 (3,27)	40	69 (2.16)	68 (4,84)
0,50	110 (3.45)	94 (6,69)	47	925 (29.0)	331 (23,54)
0,80	443 (13.9)	408 (29,02)	50	1704 (53.4)	553 (39,33)
Total	3191	1406	Total	3191	1406

#### 4. Median Ratios and Variability

To compare the results obtained from the different parameters in a fast, simple and straightforward way, the ratios between the parameters have been used. These ratios can be useful for improving existing attenuation laws [4], for instance by just multiplying them by the median ratios. Two different kinds of ratios are shown in this section. The first one is related to the median response (percentile 50) and are similar to  $S_{a_{GMAR}}$ ; the second one holds for the maximum response (percentile 100) including, in this group, the proposed parameter  $S_{RSS}$ , related to root-sum-of-squares.

In the case of the median response spectra, for each record it is necessary to determine the following 5 response spectra:  $S_{a_{GMAR}}$ ,  $S_{a_{GMROTD50}}$ ,  $S_{a_{GMROTI50}}$ ,  $S_{a_{ROTD50}}$  and  $S_{a_{ROTI50}}$ . Once the 1406 spectra have been calculated, four ratios are considered dividing the four last spectra by the first one ( $S_{a_{GMAR}}$ ). It is noteworthy that this procedure implies the computation of a total of 379 620 response spectra. This leads to 1406 values for each ratio and for each considered period (remember that depending on the  $F_L$  of the Table 2, this number decreases as the period increases), being necessary then to perform an average to obtain the desired results. The distribution of the different response spectra and its ratios, follow a lognormal distribution and therefore the mean values correspond to the antilog of the mean of the logarithmic value of the relationship. A similar procedure has been used by other authors [4,17,18]. In the same sense, the standard deviation corresponds to the normal standard deviation of the logarithm of the ratios and, if the confidence intervals are examined, it is necessary to calculate first the log value of the ratio, then to do the addition or subtraction processes and finally, to compute the antilog of the result.

The results obtained for the DB-01 are shown in Fig. 4. As it was expected, ratios are close to one, but over the period range the  $S_{a_{GMROt}}$  are more similar to the  $S_{a_{GMAR}}$ . As the period increases,  $S_{a_{ROTD50}}$  and  $S_{a_{ROTI50}}$  reach values between a 4 and 6 percent higher than the  $S_{a_{GMAR}}$ . In general, the ratios with the period dependent spectra ( $S_{a_{GMROTD50}}$  and  $S_{a_{ROTD50}}$ ) show a lower standard deviation compared with the independent spectra ( $S_{a_{GMROTI50}}$  and  $S_{a_{ROTI50}}$ ). This fact can be related to the fact that the independent spectra are, on average, an approximation of the dependent one but, for some range of periods this approximation could be not appropriate (as was shown in Fig. 1) and a large dispersion can exist. This phenomenon is especially noticeable in the  $S_{a_{ROTI50}}/S_{a_{GMAR}}$  ratio, where the deviation is twice as the obtained for the other ratios.

The maximum response parameters  $S_{a_{GMROTD100}}$ ,  $S_{a_{GMROTI100}}$ ,  $S_{a_{ROTD100}}$  and  $S_{a_{ROTI100}}$  were calculated with the same response spectra used to calculate the previous IMs; in this case, instead of the 50<sup>th</sup> percentile the 100<sup>th</sup> percentile (or the maximum value) was selected for each record. Moreover, the  $S_{RSS}$  is obtained separately as it requires computing 2812 response spectra, only two for each record, for the entire database DB-01.

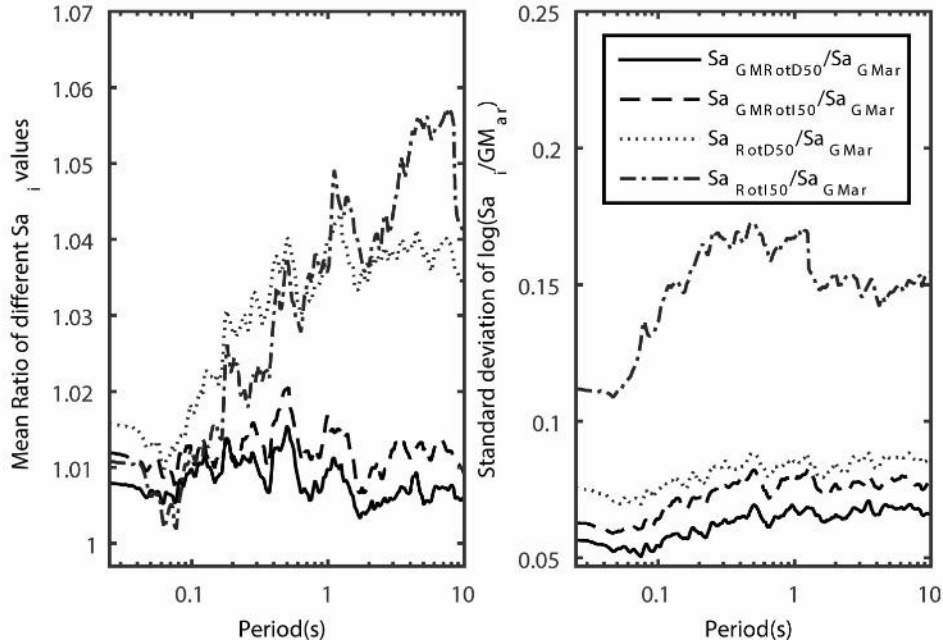


Fig. 4 – Mean value and standard deviation for different median response spectra for DB-01.

The ratios between the 100<sup>th</sup> percentile IM and  $Sa_{GMar}$ , are shown in Fig. 5. The  $Sa_{GMrot}$  ratios exhibit a flat behavior and the differences with respect to  $Sa_{GMar}$  are around 4 and 7%. This low error values are due to the fact that these measures are based on a similar averaging method, that is, the geometric mean of the response spectra projections. In the case of the  $Sa_{RotD100}$ ,  $Sa_{Rot100}$  and  $Sa_{RSS}$ , the amplification of the response is around 15% for  $Sa_{Rot100}$  and between 22 and 31% for the other two parameters respectively. As it can be seen in this figures, the lines corresponding to the ratios of  $Sa_{RotD100}$  and  $Sa_{RSS}$  are overlapped because the difference between them are very small due to the small rotation angle increment chosen for the computation of rotated response spectra ( $\Delta\theta = 1^\circ$ ).

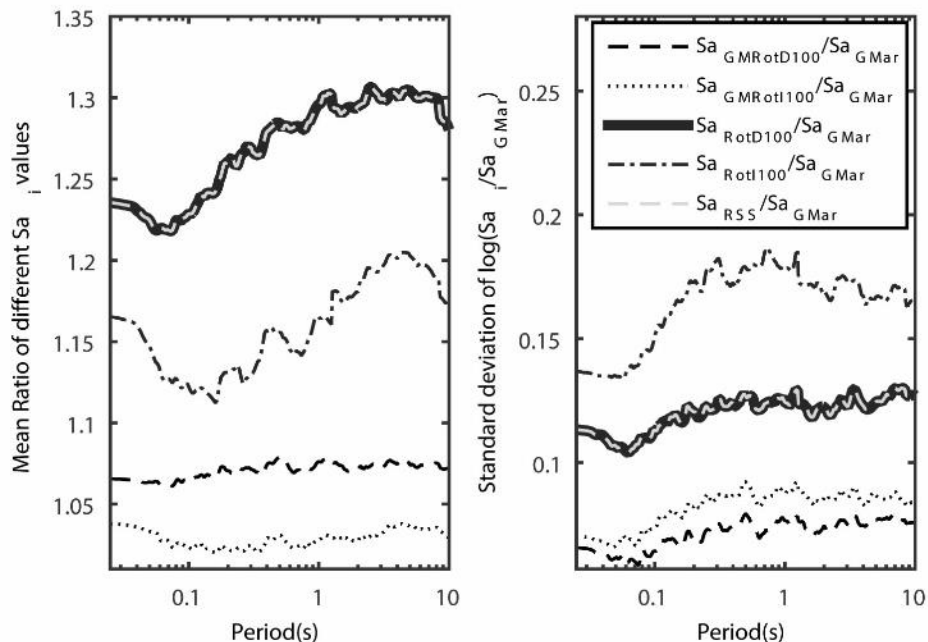


Fig. 5 – Mean values and their standard deviation of the ratios of 100<sup>th</sup> percentile IM and  $Sa_{RSS}$  for DB-01.

To obtain the  $Sa_{RotDpp}$ , a verification of the response of a SDOF is made for several possible sensor orientations spaced  $\Delta\theta$  degrees. If this  $\Delta\theta$  is small enough, we can find the orientation in which the maximum response occurs (i.e.,  $Sa_{RotD100}$ ). Otherwise, if a large  $\Delta\theta$  is employed, the possibility of reaching this solution decreases and it can differ from  $Sa_{RSS}$ . Similar comments can be stated for the standard deviations. Moreover, the standard deviations are higher for the period independent response spectra than for the period dependent ones. The ratios of the maximum response spectra exhibit an increasing tendency for interim periods with two semi-flat regions, the first one in the low period range ( $T_n < 0.2s$ ) and the second one in the high period zone ( $T_n > 2.0s$ ). Similar results were obtained by Beyer and Boomer [4] for the NGA database, with a slight lower dispersion in the ratios of maximum responses.

The 2008 NGA attenuation laws, were done to predict the  $Sa_{GMROI50}$  at a site [8]. After this, the  $Sa_{RotDpp}$  was proposed as IM for seismic hazard analysis by NEHRP [19], in particular the  $Sa_{RotD100}$  (considering the maximum response spectrum) is considered to be a more reliable parameter for the structural design. The use of maximum parameters as input in seismic hazard studies must take into account the variation in the probability of exceedance of the ground motion in order to maintain a constant risk level in the analyzed region. The application of a straightforward transformation between any kind of IM, as a way to modify the seismic hazard for assessment of structures, could derive in a non-uniform hazard level in the zones where the attenuation law is applied [20].

Finally, the relationship between the maximum response parameter ( $Sa_{RotD100}$  or  $Sa_{RSS}$  in the case of this research) and the  $Sa_{GMROI50}$  allows us to compare the results from different research articles and databases, as well as to verify if there exists any variation in their behavior. Fig. 6 shows a comparison between the corresponding ratio  $Sa_{RSS}/Sa_{GMROI50}$  as obtained in this paper and the ones obtained from other studies and databases [4,17,19,21,22,23]. As it can be seen in this figure, the results obtained in this paper present a similar behavior with the other curves, except for the last fragment. The first part of the curve is flat around a value of 1.22, until around 0.15 seconds, after that, the curve increases to 1.28 at 1.0 second period, being flat again after that. This last segment of the curve differs from other studies because, in our case, it lacks of an increment in the high period zone ( $T_n > 4s$ ). This phenomenon could be due to the absence of far field (FF) records in our database, because of the narrowness of Central America or to instabilities of these procedures for long periods

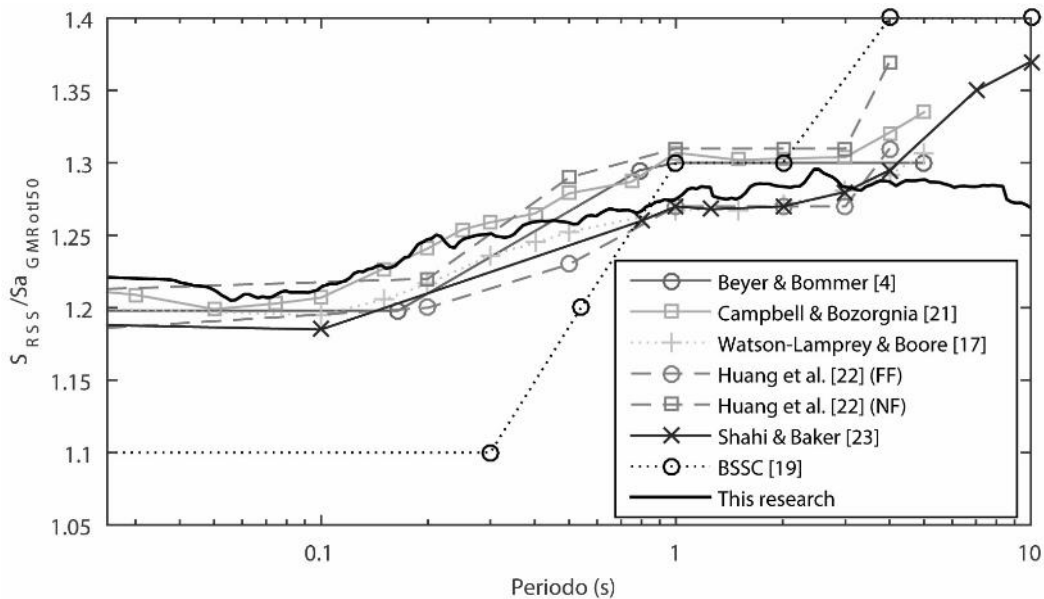


Fig. 6 – Mean value of the ratio  $Sa_{RSS}/Sa_{GMROI50}$  for DB-01 and other research.

All the databases in general, show an increment in the dispersion of data in the high period zone (above 4 seconds). This fact can be related to the deficiency of reliable data for high periods due to the fact that filtering

can produce loss of information from high magnitude and intensity records corresponding to older events. In our database DB-01, about 35.71% of the records were excluded of the analysis for periods greater than 4 seconds (0.25Hz) according to the low frequency cut values shown in Table 2.

## 5. Discussion

The application of a new intensity measure of the maximum response proposed here, has shown that it can be a more realistic and efficient way to define the maximum expected seismic actions instead of the  $Sa_{RotD100}$  proposed by Boore [6], giving as well a physical interpretation of the acceleration response of a SDOF system when submitted to two horizontal orthogonal accelerograms. The use of this parameter is promising, since the design standards are just starting to include it and not only for the determination of the attenuation laws, but also for the selection of records to be used in time history dynamic analyses [24].

Parameters based in the geometric mean ( $Sa_{GMar}$ ,  $Sa_{GMRotDpp}$ ,  $Sa_{GMRotlpp}$ ), as analyzed in our database, have shown similar behaviors, like being constant and independent from the period. In the case of the 50<sup>th</sup> percentile the values are close to the as-recorded, being only about 1-2% higher than the  $Sa_{GMar}$ . In the case of the 100<sup>th</sup> percentile, the values are in the range between 4 and 7% higher than the as-recorded. Standard deviations show a dependence on the period, with an increment between 0.1 and 1 seconds and a flat behavior outside this limits. Single component rotation parameters ( $Sa_{RotDpp}$  and  $Sa_{Rotlpp}$ ) show also a dependence on the period, increasing in the range from 0.1 to 1 second. The median value ( $Sa_{RotD50}$  and  $Sa_{Rotl50}$ ) begins near the same ordinate as  $Sa_{GMRot}$  and reaches maximum values of 4 and 6 percent higher than the  $Sa_{GMar}$  values. The maximum response spectra (percentile 100 and  $Sa_{RSS}$ ) present a similar behavior but with an important increase in the values, reaching values above 1.30 times than  $Sa_{GMar}$ .

The  $Sa_{RotD100}$  spectrum can be considered an approximation of  $Sa_{RSS}$  spectrum; moreover, differences between  $Sa_{RSS}$  and  $Sa_{RotD100}$  diminish when the angle increment ( $\Delta\theta$ ) used to compute the rotated components decrease. Thus, it is concluded that both  $Sa_{RotD100}$  and  $Sa_{RSS}$  are equivalent. The maximum response spectrum has a greater deviation with respect to the  $Sa_{GMar}$  than response spectra based on the median response, and this significant increment in the dispersion may affect the regression process for new attenuation laws that may use this response spectrum as IM of the seismic actions. It is worth to comment, that this kind of ratios and their possible application to transform spectral amplitudes do not intend to substitute existing PSHA results but, certainly they must be kept in mind for future research.

Results obtained for the Central American database are consistent with the ones obtained by others by using other databases. Using a broader database, containing all the available records, has pros and cons, as this may affect the obtained results. Using more records may allow reducing the dispersion, especially in the long period zone, where many records have been discarded. The records used in this work can be separated according to different criteria and/or classified in order to be used in other specific studies as, for instance, to obtain soil dependent response spectra or to analyze other specific variables as functions of magnitude or epicentral distance.

## 6. Conclusions

This paper shows the main results of a study about the directionality effects on the computation of acceleration response spectra. An extensive database of accelerograms recorded in the southern part of Central America has been analyzed. Median and maximum response spectra independent of the rotation angle have been computed. In turn, period dependent and period independent measures have been also calculated for both median (50<sup>th</sup> percentile) and maximum (100<sup>th</sup> percentile) response spectra. Then, the obtained median and maximum response spectra were compared with the most used measure in predictive attenuation laws, that is the geometrical mean of the as-recorded accelerograms ( $Sa_{GMar}$ ). Moreover, the root-sum-of-squares ( $Sa_{RSS}$ ) is proposed as a good choice for seismic hazard analysis and seismic evaluation of structures, because it is computed in an easy and straightforward way, as, for each period, it requires only two time histories of the response of the orthogonal response components instead of the 180 time histories needed for the  $Sa_{RotD100}$ , if it is considered and angle increment of one degree ( $\Delta\theta=1^\circ$ ). Nicely, the results obtained are very similar to those obtained in other studies

by using data from other regions and with different earthquakes, showing a fair stability and a relative independence of the results obtained. Moreover, having maximum response spectra based on strong ground motions records produced by actual earthquakes, is attractive from the perspective of seismic design and evaluation of special structures and facilities. The results of this kind of studies reveal that they should have also a significant impact in the PSHA, both in the determination of the expected seismic intensities as well as in their uncertainties.

## 7. Acknowledgements

This work has been partially funded by the Spanish Government and with FEDER funds through the research project CGL2015-65913-P. The first author is partially supported by a scholarship from the OAICE (University of Costa Rica) and CONICIT (Costa Rica Government). The third author holds a PhD fellowships from the Universidad Juarez Autonoma de Tabasco (UJAT) and from the ‘Programa de Mejoramiento del Profesorado, México (PROMEP)’. The authors would like to thank also the following organizations and agencies for providing the strong-motion records: INETER (Nicaragua), SNET and UCA (El Salvador) and finally RSN-ICE and LIS-UCR (Costa Rica). The thanks are extended to Victor Schmidt, Aaron Moya and to all the personnel of LIS-UCR for compiling and providing the database from Central America 1967-2010 and for their invaluable collaboration.

## 8. References

- [1] Douglas, J. (2003) Earthquake ground motion estimation using strong-motion records: a review of equations for the estimation of peak ground acceleration and response spectral ordinates. *Earth-Science Reviews*, **61**, 43–104. [http://dx.doi.org/10.1016/S0012-8252\(02\)00112-5](http://dx.doi.org/10.1016/S0012-8252(02)00112-5)
- [2] Trifunac, M. and Brady, A. (1975) A study on the duration of strong earthquake ground motion. *Bulletin of the Seismological Society of America*, **65**, 581–626.
- [3] Joyner, W. and Boore, D.M. (1981) Peak horizontal acceleration and velocity from strong-motion records including records from the 1979 Imperial Valley, California, earthquake. *Bulletin of the Seismological Society of America*, **71**, 2011–38.
- [4] Beyer, K. and Bommer, J.J. (2006) Relationships between Median Values and between Aleatory Variabilities for Different Definitions of the Horizontal Component of Motion. *Bulletin of the Seismological Society of America*, **96**, 1512–22. <http://dx.doi.org/10.1785/0120050210>
- [5] Boore, D.M., Watson-Lamprey, J. and Abrahamson, N.A. (2006) Orientation-Independent Measures of Ground Motion. *Bulletin of the Seismological Society of America*, **96**, 1502–11. <http://dx.doi.org/10.1785/0120050209>
- [6] Boore, D.M. (2010) Orientation-Independent, Nongeometric-Mean Measures of Seismic Intensity from Two Horizontal Components of Motion. *Bulletin of the Seismological Society of America*, **100**, 1830–5. <http://dx.doi.org/10.1785/0120090400>
- [7] Rupakhety, R. and Sigbjörnsson, R. (2013) Rotation-invariant measures of earthquake response spectra. *Bulletin of Earthquake Engineering*, **11**, 1885–93. <http://dx.doi.org/10.1007/s10518-013-9472-1>
- [8] Power, M., Chiou, B., Abrahamson, N., Bozorgnia, Y., Shantz, T. and Roblee, C. (2008) An overview of the NGA project. *Earthquake Spectra*, **24**, 3–21. <http://dx.doi.org/10.1193/1.2894833>
- [9] Bozorgnia, Y., Abrahamson, N.A., Al Atik, L., Ancheta, T.D., Atkinson, G.M., Baker, J.W. et al. (2014) NGA-West2 research project. *Earthquake Spectra*, **30**, 973–87. <http://dx.doi.org/10.1193/072113EQS209M>
- [10] Schmidt-Díaz, V. (2010) Avances para estudios del riesgo sísmico a escala regional y local: aplicación a América Central y a la Bahía de Cádiz (Sur de España). Universitat Politècnica de Catalunya.
- [11] Linkimer, L., Arroyo, I., Mora, M.M., Vargas, A., Soto, G., Barquero, R. et al. (2013) EL TERREMOTO DE SÁMARA ( COSTA RICA ) DEL 5 DE SETIEMBRE DEL 2012 (Mw 7.6). Spanish. *Revista Geológica de América Central*, **49**, 73–82.
- [12] Moya, A. (2006) Nuevo Formato de Datos para el Laboratorio de Ingeniería Sísmica del Instituto de Investigaciones en Ingeniería de la Universidad de Costa Rica. *Ingeniería*, **16**, 63–74.

- [13] Schmidt-Díaz, V. (2014) Ecuaciones predictivas del movimiento del suelo para América Central, con datos de 1972 a 2010. *Revista Geológica de América Central*, **50**, 7–37.
- [14] Climent, Á., Schmidt-Díaz, V., Hernández, D.A., Cepeda, J.M., Camacho, E., Escobar, R. et al. (2007) Strong-motion monitoring. In: Alvarado GE, and Bundschuh J, editors. *Central America: Geology, Resources, and Hazards*, p. 1–25.
- [15] Akkar, S. and Bommer, J.J. (2006) Influence of long-period filter cut-off on elastic spectral displacements. *Earthquake Engineering & Structural Dynamics*, **35**, 1145–65. <http://dx.doi.org/10.1002/eqe.577>
- [16] Boore, D.M. and Bommer, J.J. (2005) Processing of strong-motion accelerograms: needs, options and consequences. *Soil Dynamics and Earthquake Engineering*, **25**, 93–115. <http://dx.doi.org/10.1016/j.soildyn.2004.10.007>
- [17] Watson-Lamprey, J. a. and Boore, D.M. (2007) Beyond SaGMRotI: Conversion to SaArb, SaSN, and SaMaxRot. *Bulletin of the Seismological Society of America*, **97**, 1511–24. <http://dx.doi.org/10.1785/0120070007>
- [18] Baker, J.W. (2011) Conditional mean spectrum: Tool for ground-motion selection. *Journal of Structural Engineering*, **137**, 322–31. [http://dx.doi.org/10.1061/\(ASCE\)ST.1943-541X.0000215](http://dx.doi.org/10.1061/(ASCE)ST.1943-541X.0000215).
- [19] BSSC. (2009) 2009 NEHRP Recommended Seismic Provisions for New Buildings and Other Structures [Internet]. Washington, D.C.
- [20] Stewart, J.P., Abrahamson, N. a., Atkinson, G.M., Baker, J.W., Boore, D.M., Bozorgnia, Y. et al. (2011) Representation of Bidirectional Ground Motions for Design Spectra in Building Codes. *Earthquake Spectra*, **27**, 927–37. <http://dx.doi.org/10.1193/1.3608001>
- [21] Campbell, K.W. and Bozorgnia, Y. (2007) Campbell-Bozorgnia NGA Ground Motion Relations for the Geometric Mean Horizontal Component of Peak and Spectral Ground Motion Parameters [Internet].
- [22] Huang, Y., Whittaker, A. and Luco, N. (2011) Establishing maximum spectral demand for performance-based earthquake engineering: collaborative research with the University at Buffalo and the USGS [Internet]. Reston, Virginia.
- [23] Shahi, S.K. and Baker, J.W. (2013) NGA-West2 Models for Ground-Motion Directionality. Berkeley.
- [24] BSSC. (2015) NEHRP Recommended Seismic Provisions for New Buildings and Other Structures, FEMA P-1050 [Internet]. Federal Emergency Management Agency.